Liquid Crystals
Publication details, including instructions for authors and subscription information:
http://www.informaworld.com/smpp/title~content=t713926090

Ferroelectric, pyroelectric and electro-optic properties of a chiral side chain copolymer with high polarization and a broad C* phase

B. Helgee[a]; T. Hjertberg[a]; K. Skarp[b]; G. Andersson[b]; F. Gouda[b]
[a] Department of Polymer Technology, Chalmers University of Technology, Göteborg, Sweden [b] Department of Physics, Chalmers University of Technology, Göteborg, Sweden

To cite this Article Helgee, B. , Hjertberg, T. , Skarp, K. , Andersson, G. and Gouda, F.(1995) 'Ferroelectric, pyroelectric and electro-optic properties of a chiral side chain copolymer with high polarization and a broad C* phase', Liquid Crystals, 18: 6, 871 — 878
To link to this Article: DOI: 10.1080/02678299508036705
URL: http://dx.doi.org/10.1080/02678299508036705

LIQUID CRYSTALS, 1995, VOL. 18, NO. 6, 871–878

Ferroelectric, pyroelectric and electro-optic properties of a chiral side chain copolymer with high polarization and a broad C* phase

by B. HELGEE* and T. HJERTBERG
Department of Polymer Technology, Chalmers University of Technology, S-412 96 Göteborg, Sweden

K. SKARP, G. ANDERSSON and F. GOUDA
Department of Physics, Chalmers University of Technology, S-412 96 Göteborg, Sweden

(*Received 8 September 1994; accepted 23 November 1994*)

The synthetic route to a chiral side chain copolymer exhibiting broad smectic phases is described. The copolymer shows a smectic C* phase from below room temperature up to 105°C. Ferroelectric properties of this copolymer are reported as well as results showing electroclinic switching. The pyroelectric effect and the dielectric behaviour of the copolymer are also demonstrated.

1. Introduction

The successful demonstration of ferroelectric liquid crystallinity in polymers is a rather recent development in polymer science [1]. The first reported polymers were difficult to align and not electro-optically active. In recent years however, several new structures have been reported [2–8], many of which show both smectic A* and C* phases. Apart from synthetic achievements concerning novel side chain concepts, and new polymer main chains, the potential uses of these new polymeric materials in a number of application areas have been demonstrated. However, several basic questions are still open, for example, concerning main chain side chain interactions, elastic properties of the side chain mesophase and microphase separation phenomena. Therefore, continued work to establish structure property relationships in ferroelectric liquid crystalline (FLC) polymers is of vital importance for further progress in the field, both for basic understanding and use in technical applications.

The FLC systems that are described in this paper are derivatives of 4′-hydroxybiphenyl-4-carboxylic acid phenyl ester. The chiral group is a substituted lactic acid moiety. Low molar mass FLC-systems [9–11] and one case of a polymeric FLC-system [7] of similar chemical structure have been described earlier. Our studies on the FLC systems **I** (side chain precursor) and **II** (side chain copolymer) will be followed by a series of studies on liquid crystalline side chain precursors and polymers with the same basic structure. In the resulting papers, the influences of substituents and substitution patterns on the liquid crystallinity and ferroelectricity of the systems will be described. The reason for choosing this type of system was that the published analogues showed a high spontaneous polarization and at the same time wide range S_C^* phases at rather low temperatures. This made them very suitable for use in side chain liquid crystalline polymers.

The resulting FLC polymer—a siloxane backbone copolymer—shows a very broad smectic C* phase and high spontaneous polarization. The measured data on spontaneous polarization, tilt angle and response times of the copolymer are compared with the data on the mesophase of the pure side chain precursor. The properties are also compared with a low molar mass FLC of similar structure. Electric field induced tilt angles and response times for the electroclinic effect in the A* phase are also reported.

* Author for correspondence.

2. Experimental

2.1. *Materials*

Reagents and solvents used in this work are of commercial grade quality and have been used without further purification unless otherwise noted. Dry solvents were prepared by passing the solvent through a column of ICN Alumina N-Super 1 obtained from ICN Biochemicals GmbH, Germany. NMR spectra have been recorded on a Varian VXR300S or a Varian XL400 spectrometer.

0267–8292/95 $10·00

Optical activity was determined using a Perkin–Elmer 241 polarimeter. Melting points were determined using an Olympus microscope equipped with a Mettler hot stage. Phase transitions have been recorded using a Perkin–Elmer DSC-7.

2.2. *Synthesis*

2.2.1. (+)(*R*)-2-(4-*Hydroxyphenoxy*)*propanoic acid butyl ester* (*See schemes 1 and 2 of figure 1*)

Hydroquinone monobenzoate was synthesized and recrystallized from ethanol/water, m.p. 161–3°C (lit. [12] 161°C). In order to prepare (+)(*R*)-2-(4-benzoyloxyphenoxy)propanoic acid ethyl ester 8 g (37·4 mmol) of hydroquinone monobenzoate, 4·4 g (37·4 mmol) of (−)(*S*)-ethyl lactate and 12·7 g (48·6 mmol) of triphenylphosphine were dissolved in 100 ml of dried tetrahydrofuran. Diethyl azodicarboxylate (8·5 g, 48·6 mmol) was added drop by drop. The reaction mixture was left stirring overnight, whereupon the solvent was removed under vacuum. The residue was dissolved in ethyl acetate and the triphenylphosphine oxide precipitated by the addition of petroleum ether and filtered off. The filtrate was chromatographed on silica gel using ethyl acetate/petroleum ether, 1/4 as eluent. The product, obtained as an oil in 78 per cent yield (9·1 g, 29 mmol), was hydrolysed by stirring over a weekend in a mixture of 6 g of potassium hydroxide, 100 ml of ethanol and 10 ml of water. The solution was acidified and the organic solvent evaporated. The remaining aqueous phase was shaken with methylene chloride to remove benzoic acid, followed by extraction into ether of the 2-(4-hydroxyphenoxy)propanoic acid in 65 per cent yield (3·5 g, 19 mmol) ^{1}H NMR in DMSO-d_6 δ 1·42 (d, 3 H), 4·62 (q, 1 H), 6·67 (m, 4 H).

The acid was esterified in butan-1-ol using hydrogen chloride gas. The butan-1-ol was evaporated off and the residue was taken up in ether, washed with water, dried over magnesium sulphate and chromatographed on silica gel using ethyl acetate/petroleum ether, 1/4 as eluent. A pure clear oil resulted. Yield 80 per cent (3·6 g, 15 mmol); overall yield 40 per cent. $[\alpha]_D^{22} = +39{\cdot}8°$ ($CHCl_3$). ^{1}H NMR in $CDCl_3$ δ 0·9 (t, 3 H), 1·3 (m, 2 H), 1·6 (d + m, 5 H), 4·15 (m, 2 H), 4·65 (q, 1 H), 6·72 (m, 4 H).

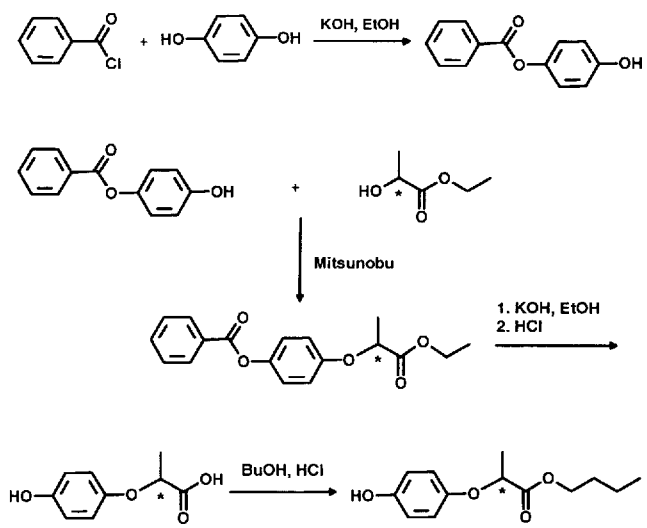

Scheme 1

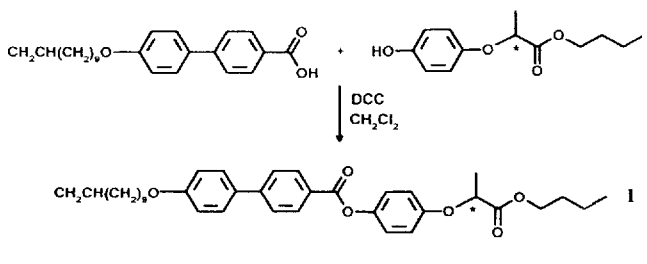

30°C S_C^* 74°C S_A 106°C I

Scheme 2

Figure 1. Synthesis schemes 1 and 2.

2.2.2. 4′-(*Undec-10-enyloxy*)*biphenyl-4-carboxylic acid*

4′-Hydroxybiphenyl-4-carboxylic acid was synthesized and etherified with undec-10-enyl bromide according to [13] and [14], respectively, yielding 4′-(undec-10-enyloxy)biphenyl-4-carboxylic acid. m.p. 160°C; LC phase–isotropic at 230°C. ^{1}H NMR in DMSO-d_6/$CHCl_3$ mixture, δ 0·8–1 (m, 12 H) 1·3 (quintet, 2 H), 1·55 (q, 2 H), 3·5 (t, 2 H), 4·45 (m, 2 H), 5·3 (m, 1 H), 6·48 (d, 2 H), 7·08 (d, 2 H), 7·14 (d, 2 H), 7·55 (d, 2 H).

2.2.3. (+)(*R*)-4′-(*Butoxycarbonyl-1-ethoxy*)*phenyl* 4-[4-(*undec-10-enyloxy*)*phenyl*]*benzoate* (**I**)

1·1 g (3·0 mmol) of 4′-(undec-10-enyloxy)biphenyl-4-carboxylic acid, 1·43 g (6 mmol) of (+)(*R*)-2-(4-hydroxyphenoxy)propanoic acid butyl ester and 10 mg of 4-(*N*,*N*-dimethylamino)pyridine were dissolved in 50 ml of dry methylene chloride. The mixture was cooled in an ice bath and 0·75 g (3·6 mmol) of dicyclohexylcarbodiimide was added. The reaction mixture was allowed to reach room temperature and was left stirring over night. To isolate the product, the urea formed was filtered off and the solvent evaporated. The residue was recrystallized from ethanol and the pure product was isolated in 68 per cent yield. $[\alpha]_D^{22} = +18{\cdot}0°$($CHCl_3$). ^{1}H NMR in $CDCl_3$, δ 0·9 (t, 3 H), 1·2–1·5 (m, 14 H), 1·6 (d + m, 5 H), 1·8 (quintet, 2 H), 2·04 (q, 2 H), 4·0 (t, 2 H) 4·18 (m, 2 H) 4·75 (q, 1 H), 4·95 (m, 2 H), 5·8 (m, 1 H), 6·92 (d, 2 H), 7·0 (d, 2 H), 7·12 (d, 2 H), 7·58 (d, 2 H), 7·68 (d, 2 H), 8·2 (d, 2 H).

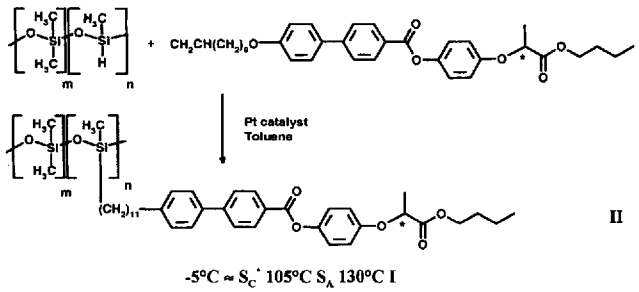

Figure 2. Scheme 3.

2.2.4. *Ferroelectric liquid crystalline side chain copolymer* (**II**) *see figure 2.*

0·59 g (1·0 mmol) of the side chain precursor (**I**) and 0·26 g (equivalent of 1·0 mmol of Si–H groups) of dimethylsiloxane–methylhydrosiloxane copolymer with a copolymer ratio 2·7/1 and a degree of polymerization of > 30 was dissolved in 10 ml of dry toluene. Dichlorodicyclopentadienylplatinum (0·08 mg) was added as catalyst at the start of the reaction. Nitrogen was bubbled through the solution and the flask was sealed with a septum and heated at 100°C. After heating the solution for 24 h, an equal amount of catalyst was added. After 48 h of heating, the polymer was precipitated in methanol. The polymer was twice redissolved in chloroform and reprecipitated in methanol. Finally the polymer was dissolved in chloroform and filtered through a 0·2 μm Teflon filter. The solvent was removed and the polymer was dried in vacuum. Yield 0·55 g (65%). $[\alpha]_D^{22} = +13{\cdot}84°(CHCl_3)$. The ^{1}H NMR spectrum of the polymer shows broader signals than those of the side chain precursor, but is otherwise very similar with the exceptions that the signals from methyl and methylene groups attached to silicon at $\delta = 0$–$0{\cdot}1$ ppm and a methylene group β to the silicon at $\delta = 0{\cdot}5$ ppm are present, while the olefinic protons at $\delta = 4{\cdot}95$ ppm and $\delta = 5{\cdot}8$ ppm are absent. A Si–H signal appeared at $\delta = 4{\cdot}7$ ppm equivalent to 15 per cent of unreacted hydrogens.

2.3. *Sample preparation and electric measurements*

For the study of physical properties such as electro-optic or pyroelectric effects in FLC polymers, the achievement of well-aligned samples is essential. Our standard shear cell [15], built for measurements on low molar mass FLCs, has proven very useful for obtaining aligned polymer samples. The polymer sample is applied on the lower glass plate, and melted into the isotropic phase to cover the whole glass area. Then the upper glass plate is put on, and the shear cell is assembled. Orientational shear was applied in the smectic A phase. A special electrode pattern assures that the active area is always 16·8 mm^2, independent of shear position. Spacers consist of thermally evaporated 2 μm SiO_2, and the orientation of the smectic

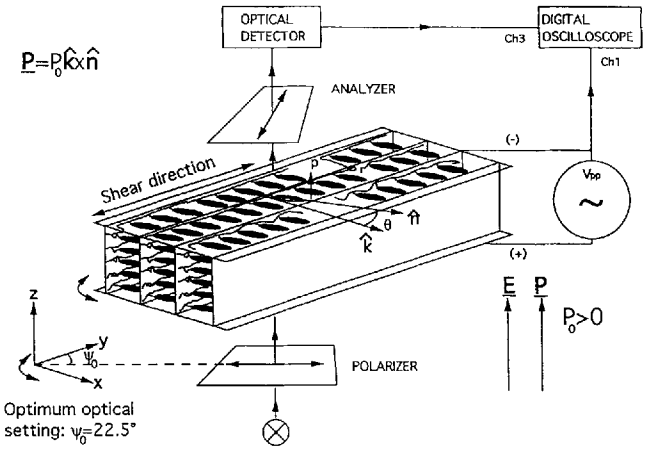

Figure 3. Experimental set-up and cell geometry.

layers is such that the layer normal is perpendicular to the shear direction, cf. figure 3. A 1000 Å protective SiO_2 layer covers the ITO electrodes. The shear alignment cell is mounted in a Mettler FP52 hot stage for temperature control and put in a Zeiss Photomicroscope for observation in crossed polarizers. The sample temperature is independently measured by a Pt 100 resistor element drilled into the sample itself. In some cases alignment could also be achieved in polyimide coated, glued cells of active area 16 mm^2 and thickness 4 μm, obtained from EHC.

The measurements of the spontaneous polarization P_s were made with either the bridge method or the triangular wave method. Contrary to the case for many FLC side chain polymers, in the case of copolymer (**II**), it was always possible, even at low temperatures (high rotational viscosity), to obtain a well defined hysteresis loop, cf. figure 4, which shows a hysteresis curve at $T = 68{\cdot}1$°C. The measured polarization curve is taken from a series of hysteresis curves, where the reading of amplitude of the

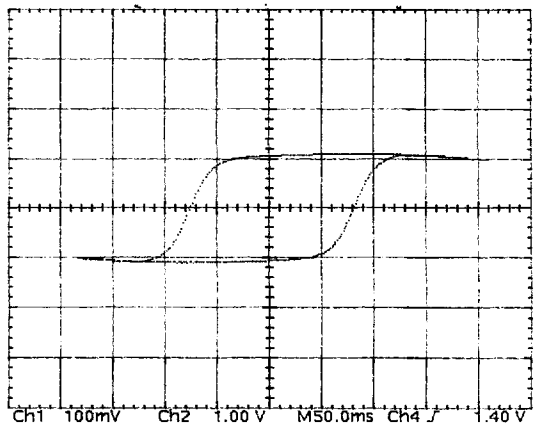

Figure 4. Ferroelectric hysteresis loop of the copolymer at $T = 68{\cdot}1$°C.

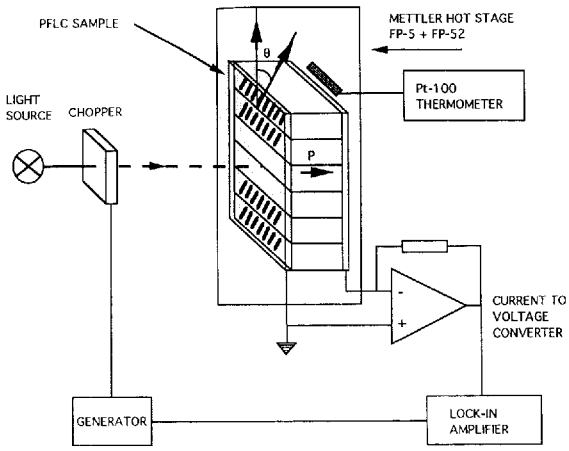

Figure 5. The experimental arrangement for pyroelectric measurements.

loop directly gives the spontaneous polarization by the equation

$$P_s = \frac{1}{2A}\frac{k\Delta U}{G}C_1$$

where A is the active sample area (16·8 mm^2), k is a correction factor for the SiO_2 protective layer ($k = 1{\cdot}1$ for the shear cell glasses), G is the gain of the instrumental amplifier, ΔU is the amplitude of the loop, and C_1 is the reference capacitor in series with the FLC polymer sample.

2.4. *Pyroelectric measurements*

The pyroelectric coefficient (γ) is defined as the temperature derivative of the spontaneous polarization. In the method exploited by Chynoweth [16], the temperature is varied periodically with an angular frequency ω. A monodomain sample of a ferroelectric material produces a pyroelectric current i of the same frequency. γ is proportional to the amplitude of i, and the spontaneous polarization can be evaluated by integrating γ:

$$i(\omega) = A\frac{dP}{dt} = A\frac{dP}{dT}\frac{dT}{dt} = A\gamma\frac{dT}{dt}, \quad P_s(T) = \int \gamma dT$$

where A is the active area of the sample, P_s is the spontaneous polarization and T is the temperature.

The technique used in the present study is a quasi-stationary method where the sample is kept at a constant average temperature, and is at the same time exposed to a rather small alternating disturbance, small in the sense that the disturbance does not change the average temperature. The periodic temperature variation is enforced on the sample by means of a chopped light beam. The sample has an active area of 4 × 4 mm^2, and a thickness of 4 μm. The sample holder is housed in a Mettler FP 52 oven and the temperature is controlled to better than 0·2°C by an FP 5 regulator unit.

The light beam from a medium power halogen lamp is focused to cover the active area of the sample (see figure 5). The beam is chopped to a pulse train by means of an ordinary rotating chopper which is synchronized to an external generator which also gives the reference signal to the lock-in detector system. The pyroelectric signal is then monitored by a current amplifier (Ortec 5005) connected to a lock-in amplifier (EG&G 5208).

2.5. *Optical and dielectric measurements*

In order to measure the smectic tilt angle Θ in the C* phase, we applied a low frequency square wave field, and determined the two extinction orientations by rotating the sample between crossed polarizers. If the sample is kept fixed at the orientation 22·5 degrees to the polarizer axis, the optical transmission curve of figure 6 is observed. Because the tilt angle exceeds 22·5 degrees, the optical transmission between crossed polarizers goes to a maximum and saturates at a lower value when the switching voltage has reversed. See [17] for a discussion of this phenomenon, and a numerical fit of the optical response in the case $\Theta > 22{\cdot}5°$.

The dielectric measurements have been carried out on the copolymer **II** in the frequency regime 10 Hz to 10 MHz. A measuring electric field of 1 V_{pp} was superimposed on the internal bias field. Due to the freely moving charges, the dielectric absorption at low frequency increases exponentially, exhibiting the so called 'conductivity tail'. In our case, the dielectric absorption, due to the conductivity tail, reaches a large value which has completely obscured the soft mode dielectric absorption peak. However, a bias electric field of 10 V/4 μm was found to decrease the conducting tail by two orders of

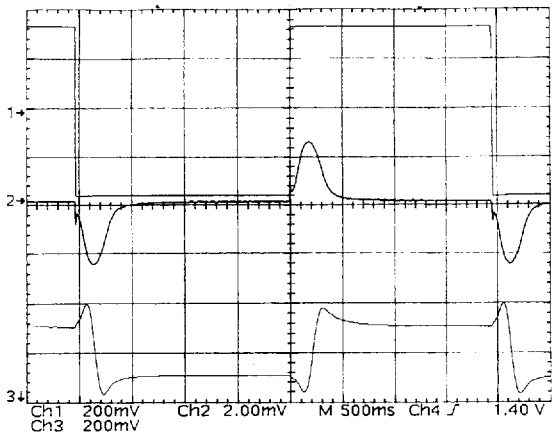

Figure 6. Optical transmission curve to an applied square wave voltage at $T = 22{\cdot}2$°C. Trace 1 = applied field, trace 2 = current response and trace 3 = optical response.

magnitude, thus enhancing the measurement resolution drastically. Furthermore, the bias field facilitates probing of the soft mode dielectric strength in the C* phase due to unwinding of the helical structure. The experimental details of dielectric relaxation spectroscopy are published elsewhere [18].

3. Results and discussion

3.1. *Synthesis*

The synthesis of the ferroelectric liquid crystalline systems is divided into three parts as already shown in schemes 1–3. First, the chiral group is synthesized via a Mitsunobu reaction of hydroquinone monobenzoate with ethyl lactate. This is performed by analogy with the alkylation of a mixed imide with ethyl lactate under Mitsunobu conditions [19]. This was shown to occur with inversion of configuration. A good yield of product with a large enantiomeric excess was obtained. Hydrolysis of the ester groups and esterification gave the desired chiral group.

The synthesis of 4′-hydroxybiphenyl-4-carboxylic acid [13] and its etherification [14] were straight forward reactions (see scheme 2).

In the final step of the side chain precursor synthesis, the biphenylcarboxylic acid was esterified with the chiral propanoic ester derivative using dicyclohexylcarbodiimide [20].

The ferroelectric liquid crystalline side chain polymer was finally obtained by a hydrosilylation reaction (see scheme 3)

3.2. *Ferroelectric properties*

The spontaneous polarization, measured with the bridge method, is plotted versus temperature in figure 7 for the copolymer **II** and for the mesogenic side chain precursor **I**. It is seen that the copolymer has a rather high polarization saturating at about 160 nC cm^{-2}, while for the side chain precursor as such we obtain, as expected, a higher value for P_S, saturating at about 300 nC cm^{-2}. A similar copolymer prepared by Naciri *et al.* [7], showed a highest polarization of 180 nC cm^{-2} at 40°C. The sign of the spontaneous polarization is defined as the sign of the vector cross product between the smectic layer normal and the director. In this case the sign of the spontaneous polarization was determined to be positive ($P_S > 0$) for both the side-chain precursor and the copolymer. A ferroelectric low molar mass liquid crystal with similar structure has been described in the literature [9]. This compound shows P_S values comparable to the values for the pure side chain precursor. Lower polarization values for the FLC polymer compared to its pure side chain have been observed in other systems, and can be interpreted as a dilution effect, lowering the number of macroscopic dipoles per unit volume.

Since the pyroelectric coefficient is proportional to dP/dT, and the measured pyroelectric current is proportional to the pyroelectric coefficient, a large pyroelectric signal should be observed close to the smectic A–C transition, where there normally is large variation in P_S. As seen in figure 7, we observe a less drastic temperature dependence for P_S of the copolymer, and consequently the pyroelectric current, figure 8, shows a less pronounced peak. In fact, the derivative dP/dT is nearly constant in the

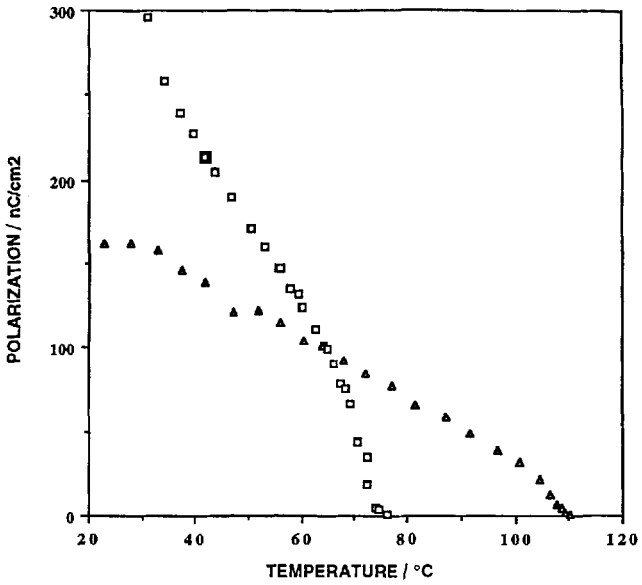

Figure 7. Spontaneous polarization versus temperature for the copolymer **II** (▲), and for the side chain precursor (□).

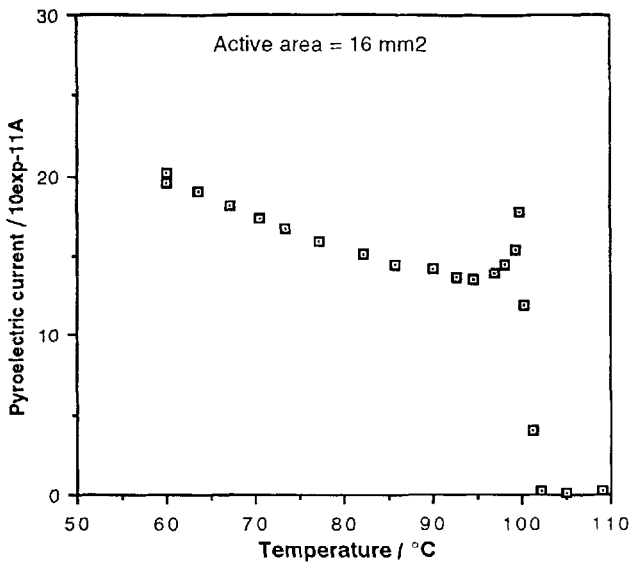

Figure 8. Pyroelectric response for copolymer **II** as a function of temperature.

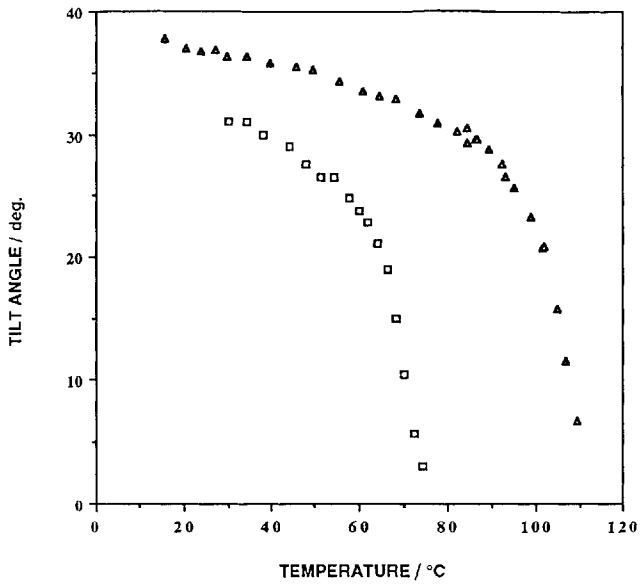

Figure 9. Tilt angle as a function of temperature for the copolymer **II** (▲), and for the side-chain precursor (□).

ferroelectric phase, giving a very weak temperature dependence for the pyroelectric signal. This is a desirable property for applications in pyroelectric sensors for example.

The title angle (Θ) for the copolymer plotted versus temperature is shown in figure 9. It is seen that very large tilt angles, up to nearly 40 degrees are obtained in this copolymer, while the side chain precursor liquid crystal see (figure 9) shows almost 5 degrees lower tilt angle values at maximum. The large values of Θ are manifested in the characteristic shape of the optical response, shown in figure 6.

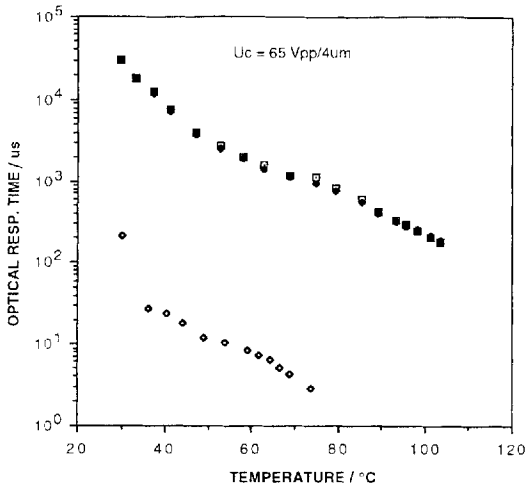

Figure 10. Response times determined from optical switching. Upper points, copolymer **II**; lower points, side chain precursor **I**.

The response time evaluated from the optical switching is shown in figure 10, for both the copolymer and its mesomorphic side chain precursor. A factor of about 100–1000 exists between these two because of the viscosity effect (the optical response time is directly proportional to the rotational viscosity of the mesogenic molecules). Such a large factor can be understood by considering different packing schemes of the mesogenic side-groups [21]. Compared to the low-molar mass situation, the side chain is rotationally constrained by its attachment through the spacer to the polymer backbone.

Electro-optical observations of the copolymer in the smectic A phase concerned the electric field induced tilt angle and response times. Electroclinic switching is observed with a response time from 6 μs at 126°C to about 100 μs at 106°C close to the A–C transition, cf. figure 11. In a comparison of our results for the electroclinic switching with those reported in [7] for a similar polymer, we find approximately the same value for the electroclinic coefficient at about 10 K above the S_A–S_C phase transition temperature, while the optical response times are about a factor of 10 shorter for copolymer **II** in the S_A phase. Values of the induced tilt angles are shown in figure 12 at different temperatures. The electroclinic coefficients (the ratio between induced tilt angle and applied field) for the copolymer are comparable to or greater than those for a commercial low molar mass electroclinic mixture (BDH 8764).

The temperature dependence of the soft mode dielectric permitivity ε' measured at different frequencies in the A* and C* phases is shown in figure 13. At the A* to C* transition temperature T_C, the dielectric behaviour exhibits

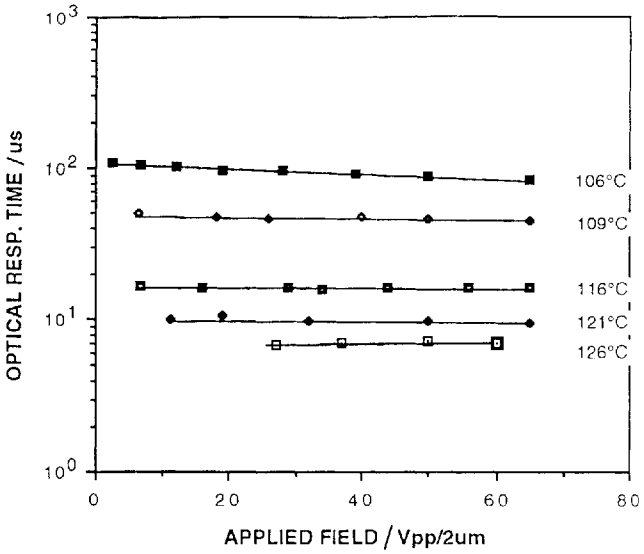

Figure 11. Response times for the electroclinic effect in the smectic A phase of copolymer **II**.

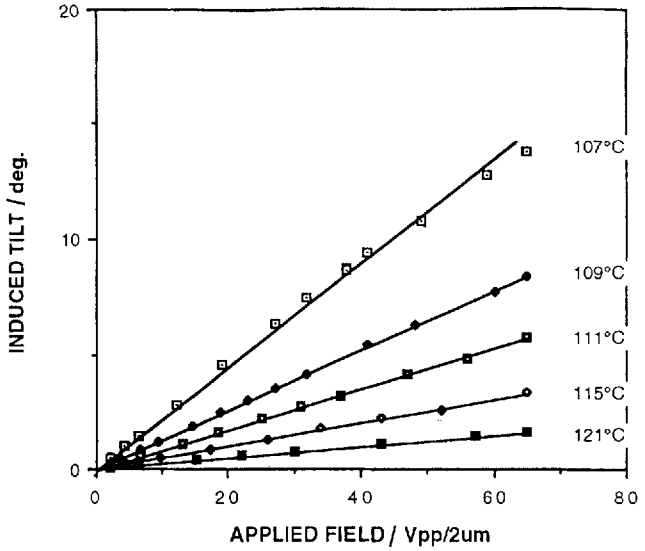

Figure 12. Field-induced tilt angles in the smectic A phase of copolymer **III**.

a cusp-like behaviour. From these measurements, T_C is found to be 95·2°C. The characteristic frequency of the soft mode f_s in the A* and C* phases is depicted in figure 14. Note that, in the C* phase, the values of f_s are shifted up from the extrapolated behaviour due to the bias electric field [18]. It is worth pointing out that the values of f_s obtained are comparable with those obtained from the response time τ of the electroclinic effect. For instance, at 106°C, $f_s \approx 10$ kHz, in good agreement with the τ value which was found to be 100 µs. Thus the dielectric and electro-optic results are in agreement with each other.

In conclusion, we have described the synthesis of a new chiral side chain copolymer, and demonstrated its

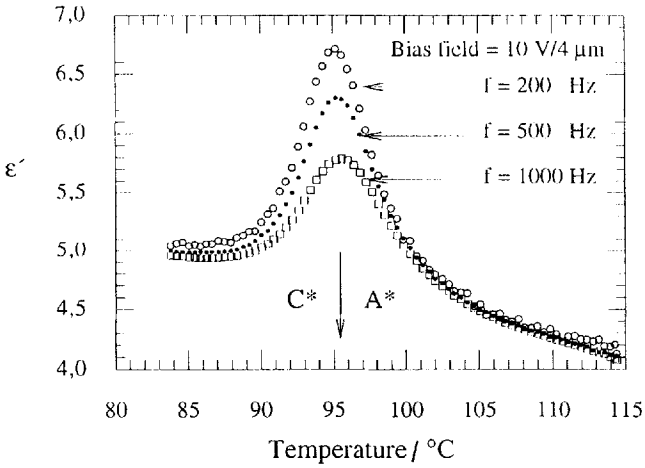

Figure 13. Temperature dependence of the soft mode dielectric permittivity measured at different frequencies for copolymer **II**.

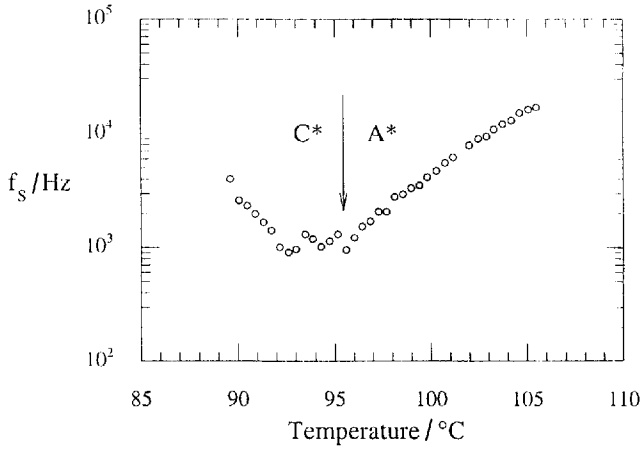

Figure 14. Temperature dependence of the soft mode relaxation frequency for copolymer **II**.

ferroelectric, pyroelectric and electro-optic properties. Main features of the polymer are an extremely broad smectic C* phase and readily achievable alignment, both for homeotropic and bookshelf cells. The copolymer exhibits large values for the spontaneous polarization and tilt angle. Several other physical properties of this interesting copolymer, such as its detailed dielectric and non-linear optical behaviour, will be reported separately.

Financial support from The Swedish Natural Science Research Council, The Swedish Technical Science Research Council and The Swedish National Board for Industrial and Technical Development is gratefully acknowledged.

References

[1] Shibaev, V. P., Kozlowskii, M. V., Beresnev, L. A., Blinov, L. M., and Platé, N. A., 1984, *Polym. Bull.*, **12**, 299.

[2] Uchida, S., Morita, K., Miyoshi, K. Kashimoto, K., and Kawasaki, K., 1988, *Molec. Crystals liq. Crystals*, **155**, 93.

[3] Zentel, R., Reckert, G., Sauvarop, B., and Kapitza, H., 1989, *Makromolek. Chem.*, **190**, 2869.

[4] Scherowsky, G., Schliwa, A., Springer, J., Kuehnpast, K., and Trapp, W., 1989, *Liq. Crystals*, **5**, 1281.

[5] Kitazume, T., Ohnogi, T., and Ito, J., 1990, *J. Am. chem. Soc.*, **112**, 6608.

[6] Dumong, M., Nguyen, H. T., Mauzac, M., Destrade, C., Arachard, M. F., and Gasparoux, H., 1990, *Macromolecules*, **23**, 355.

[7] Naciri, J., Pfeiffer, S., and Shashidhar, R., 1991, *Liq. Crystals*, **10**, 585.

[8] Svensson, M., Helgee, B., Hjertberg, T., Hermann, D., and Skarp, K., 1993, *Polym. Bull.*, **31**, 167.

[9] Taniguchi, H., Ozaki, M., Yoshino, K., Satoh, K., and Yamasaki, N., 1988, *Ferroelectrics*, **77**, 137.

[10] Jackson, D. A., and Gemmel, P. A., 1988, European Patent No. 259995 A1.

[11] OZAKI, M., UTSUMI, M., GOTOU, T., MORITA, Y., DAIDO, K., SADOHARA, Y., and YOSHINO, K., 1991, *Ferroelectrics*, **121,** 259.
[12] ROBERTSON, A., and WATERS, R. B., 1930, *J. chem. Soc.*, 2729.
[13] PERCEC, V., ZHENG, Q., and LEE, M., 1991, *J. mater. Chem.*, **1,** 611.
[14] GRAY, G. W., HARTLEY, J. B., and JONES, B, 1955, *J. chem. Soc*, 1412.
[15] SKARP, K., and ANDERSSON, G., 1986, *Ferroelectrics Lett.*, **6,** 67.
[16] CHYNOWETH, A. G., 1956, *J. appl. Phys.*, **27,** 78.
[17] POTHS, H., ZENTEL, R., HERMANN, D., ANDERSSON, G., and SKARP, K., 1993, *Ferroelectrics*, **148,** 285.
[18] GOUDA, F., SKARP, K., and LAGERWALL, S. T., 1991, *Ferroelectrics*, **113,** 165.
[19] MORIMOTO, H., FURUKAWA, T., MIYAZIMA, K., and MITSUNOBU, O., 1973, *Chem. Lett.*, 821.
[20] NEISES, B., and STEGLICH, W., 1978, *Angew. Chem.*, **90,** 556.
[21] SHIBAEV, V. P., and PLATÉ, N. A., 1984, *Advances in Polymer Science 60/61*, edited by M. Gordon (Springer-Verlag, Berlin), p. 173.